HHS Public Access

Author manuscript

J Muscle Res Cell Motil. Author manuscript; available in PMC 2016 June 01.

Published in final edited form as:

J Muscle Res Cell Motil. 2015 June ; 36(3): 243–253. doi:10.1007/s10974-015-9410-8.

Distinct muscle apoptotic pathways are activated in muscles with different fiber types a rat model of critical illness myopathy

Benjamin T. Barnes[1,*], **Amy L. Confides**[2,*], **Mark M. Rich**[3], and **Esther E. Dupont-Versteegden**[2]

[1]College of Arts and Sciences, College of Health Sciences, University of Kentucky, Lexington, KY 40536-0200

[2]Division of Physical Therapy, Department of Rehabilitation Sciences, College of Health Sciences, University of Kentucky, Lexington, KY 40536-0200

[3]Department of Neuroscience, Cell Biology and Physiology, Wright State University, Dayton, OH 45435

Abstract

Critical illness myopathy (CIM) is associated with severe muscle atrophy and fatigue in affected patients. Apoptotic signaling is involved in atrophy and is elevated in muscles from patients with CIM. In this study we investigated underlying mechanisms of apoptosis-related pathways in muscles with different fiber type composition in a rat model of CIM using denervation and glucocorticoid administration (denervation and steroid-induced myopathy, DSIM). Soleus and tibialis anterior (TA) muscles showed severe muscle atrophy (40–60% of control muscle weight) and significant apoptosis in interstitial as well as myofiber nuclei that was similar between the two muscles with DSIM. Caspase-3 and −8 activities, but not caspase-9 and −12, were elevated in TA and not in soleus muscle, while the caspase-independent proteins endonuclease G (EndoG) and apoptosis inducing factor (AIF) were not changed in abundance nor differentially localized in either muscle. Anti-apoptotic proteins HSP70, −27, and apoptosis repressor with a caspase recruitment domain (ARC) were elevated in soleus compared to TA muscle and ARC was significantly decreased with induction of DSIM in soleus. Results indicate that apoptosis is a significant process associated with DSIM in both soleus and TA muscles, and that apoptosis-associated processes are differentially regulated in muscles of different function and fiber type undergoing atrophy due to DSIM. We conclude that interventions combating apoptosis with CIM may need to be directed towards inhibiting caspase-dependent as well as -independent mechanisms to be able to affect muscles of all fiber types.

Keywords

atrophy; apoptosis; caspase; EndoG; AIF; ARC

Corresponding Author: Esther Dupont-Versteegden, Ph.D., Div. Physical Therapy, College of Health Sciences, University of Kentucky, 900 S Limestone, CTW204L, Lexington, KY 40536-0200, eedupo2@uky.edu, tel: (859) 218 0592, fax: (859) 323 6003.

*authors contributed equally to this work

Introduction

Critically ill patients in the intensive care unit (ICU) suffer frequently from a myopathy in which there is severe muscle atrophy, a syndrome now known as critical illness myopathy (CIM) (Bolton 2005; Lacomis et al. 2000; Stevens et al. 2009) This myopathy is one contributor to a syndrome of ICU acquired weakness (ICUAW), which causes severe long-term disability (Batt et al. 2013). Some of the muscle wasting and weakness associated with this syndrome may be the result of the primary disease of the patients, but interventions and treatments used in the ICU are likely important contributors. Treatments which likely contribute to development of CIM include prolonged mechanical ventilation, immobilization, and treatment with corticosteroids (Bolton 2005; Latronico and Bolton 2011; Stevens et al. 2009).

Pathological mechanisms contributing to weakness in affected patients include selective loss of myosin, severe muscle atrophy, disorganization of sarcomeres, and a lack of electrical excitability of the muscles. The underlying cellular mechanisms that lead to these abnormalities are the subject of current investigations and are thought to involve the activation of the major proteolytic pathways in skeletal muscle (ubiquitin/proteasome, autophagy/lysosome, calpain), as well as the TGF-β/MAPK cascade (Banduseela et al. 2009; Di Giovanni et al. 2004; Helliwell et al. 1998; Llano-Diez et al. 2011; Showalter and Engel 1997). Another process that has been shown to be elevated in CIM is that of apoptosis, since apoptotic morphological features as well as increases in the caspase cascade have been observed in afflicted muscles (Di Giovanni et al. 2000; Di Giovanni et al. 2004; Llano-Diez et al. 2011; Mozaffar et al. 2007). Even though the importance of apoptosis in the loss of myonuclei during disuse atrophy has recently been challenged (Bruusgaard et al. 2012; Bruusgaard and Gundersen 2008; Gundersen and Bruusgaard 2008), the involvement of apoptosis-associated pathways with muscle breakdown during aging, cancer, cachexia, haemolysis, obesity, and burn-related atrophy is becoming more accepted (Boivin et al. 2010; Sakuma and Yamaguchi 2012; Sishi et al. 2011; Smuder et al. 2010; van Royen et al. 2000; Yasuhara et al. 2000). In particular, caspase-3 activation has been shown to be an early mediator of muscle degradation and to work synergistically with the ubiquitin-proteasome system to induce muscle breakdown (Du et al. 2004; Wang et al. 2010). Moreover, caspase-3 and calpain are both involved in diaphragm muscle atrophy observed during mechanical ventilation (Nelson et al. 2012), and caspase activation is also responsible for muscle wasting induced by the proinflammatory cytokine TWEAK (Bhatnagar et al. 2012). In addition, caspase-8 has been shown to be involved in muscle atrophy in response to high glucose, TNFα and angiotensin II administration, supposedly through the activation of RNA-dependent protein kinase PKR (Eley et al. 2008; Russell et al. 2009). This indicates that caspase-dependent pathways likely play a role in muscle wasting; indeed, inhibition of caspases protects from muscle damage and atrophy (Talbert et al. 2013; Teng et al. 2011). In addition to caspase-dependent apoptotic processes, there are also caspase-independent pathways implicated in the loss of muscle mass. Endonuclease G (EndoG) and apoptosis inducing factor (AIF) are mitochondrial proteins capable of inducing apoptosis when released from the mitochondria and translocating from the cytoplasm to the nucleus (reviewed in (Dupont-Versteegden 2005; Quadrilatero et al. 2011)) and EndoG has been

shown to be specifically involved in myonuclear apoptosis (Dupont-Versteegden et al. 2006). On the other hand, skeletal muscle also contains anti-apoptotic proteins, such as heat shock proteins (HSPs) and apoptosis repressor with CARD domain (ARC), which increase in muscle during differentiation and are thought to protect the muscle from apoptosis during caspase activation (Xiao et al. 2011). The balance of these pathways will determine the extent of apoptotic signaling in a particular muscle and consequently the loss of muscle protein and fibers.

To investigate the role of apoptosis in CIM we utilized a well documented and accepted rat model which was first developed over 20 years ago and involves pairing loss of muscle activity (by denervation) with systemic administration of corticosteroids: denervation and steroid-induced myopathy (DSIM) (Massa et al. 1992; Rouleau et al. 1987). The model was established to mimic the situation in patients given systemic neuromuscular blocking agents, in conjunction with high doses of corticosteroids and it recreates all pathological findings present in CIM in patients: 1) dramatic atrophy of muscle fibers (Kraner et al. 2011; Massa et al. 1992; Mozaffar et al. 2007; Rouleau et al. 1987), 2) selective loss of myosin (Kraner et al. 2011; Massa et al. 1992; Mozaffar et al. 2007; Rouleau et al. 1987), 3) disorganization of sarcomeres (Kraner et al. 2011; Massa et al. 1992), and 4) electrical inexcitability (Rich and Pinter 2001; Rich and Pinter 2003; Rich et al. 1998). In addition, the use of glucocorticoids is independently associated with apoptosis, which is the focus of our investigation (Lee et al. 2005; Orzechowski et al. 2003). The purpose of this study was to evaluate the role of apoptosis in skeletal muscle atrophy associated with DSIM, and to identify contributing cellular pathways in different muscles; we hypothesized that apoptosis is a major contributor of skeletal muscle atrophy in this model for CIM.

Materials and Methods

Animal procedures and tissue collection

All procedures on animals were performed in accordance with institutional guidelines for the care and use of laboratory animals and all protocols were approved by the Institutional Animal Care and Use Committee (IACUC) at Wright State University (Dayton, OH). Adult female Wistar rats (250–350 g body weight) were used; CIM (n=8) was induced by denervation of the hind limbs and administration of dexamethasone as described previously (Kraner et al. 2011; Rich and Pinter 2003). Briefly, rat hind limb muscles were denervated by removing a 10 mm segment of the sciatic nerve while under inhaled isoflurane anesthesia. Buprenorphine was given subcutaneously for postoperative analgesia. Dexamethasone (5 mg/kg) was administered by i.p. injections daily starting at the day of surgery and continued for 7–10 days. Control rats (n=9) were subjected to sham surgery and received daily placebo injections for 7 days. Rats were euthanized by carbon dioxide inhalation. Soleus and tibialis anterior (TA) muscles were dissected, weighed, flash frozen in liquid nitrogen, and stored at −80C until further analysis. A second set of rats (n=8) treated similarly as above was used for the immunoprecipitation experiments.

Preparation of subcellular fractions

Cytosolic and nuclear fractions from soleus and tibialis muscles were obtained using the method described (Siu et al. 2005). Briefly muscles were pulverized, and added to ice-cold lysis buffer (10 mM NaCl, 1.5 mM $MgCl_2$, 20mM HEPES, pH 7.4, 20% glycerol, 0.1%Triton X-100, 1mM DTT, 1μg/mL leupeptin, and 1mM PMSF) at 1:5 w/v ratio. The solution was then homogenized and centrifuged at 800G for 3 min at 4°C and the supernatant was respun twice at 3,500G for 5 min at 4C, collected and stored at −80°C for use as cytosolic fraction (CF) which contains also mitochondrial proteins. Pellets from all spins were collected, washed with ice cold lysis buffer, and pooled pellets were spun at 3,500g for 5 min. Supernatant was discarded and pellet resuspended in 300 μl lysis buffer and 80 μl 5M NaCL with leupeptin (1 ng/ml), aprotinin (1 ng/ml), pepstatin (2 ng/ml) and PMSF (100 ng/ml). The nuclear pellet resuspension was rotated for 1h at 4C to lyse the nuclei, and centrifuged at 20,100g for 15 min at 4C. The supernatant was collected and stored at −80C, for use as nuclear fraction (NF). Protein concentrations were determined by Bradford assay (BioRad, Hercules, CA) and purity of the nuclear and cytosolic fractions was confirmed with histone and CuZn SOD antibodies, respectively (not shown).

Cell Death ELISA

To determine DNA fragmentation, mono- and oligonucleosomal fragments were measured using the cell death ELISA kit (Roche Applied Sciences, Indianapolis, IN) as described previously (Leeuwenburgh et al. 2005; McMullen et al. 2009). Briefly, each well contained equal volumes of CF from TA or soleus muscle and the assay was performed according to the manufacturer's instructions. Colorimetric differences were measured at a wavelength of 405 nm using Spectra Max M2 Microplate reader (Molecular Devices, Sunnyvale, CA) and normalized to the amount of protein present in the sample; therefore, the apoptotic index is expressed as arbitrary density units per μg protein.

TdT-mediated dUTP nick end labeling (TUNEL) and dystrophin staining

TUNEL assay was used to identify nuclei undergoing DNA fragmentation characteristic of nuclear apoptosis and this was preceded by dystrophin staining to distinguish myofiber from interstitial nuclei, including satellite cells. Experiments were performed according to the manufacturer's instructions for the Cell Death kit (Roche Molecular Biochemicals, Pleasanton, CA) and modified as described previously (Dupont-Versteegden et al. 1999; Leeuwenburgh et al. 2005). In brief, TA and soleus muscle cross sections were cut on a cryostat (7 μm), air dried and rehydrated in phosphate buffered saline (PBS). Sections were incubated in dystrophin antibody (1:100, Vector, Burlingame, CA) overnight, followed by incubation in AlexaFluor488 goat anti-mouse secondary antibody (1:500, Invitrogen, Carlsbad, CA). Sections were further fixed in 4% paraformaldehyde at room temperature, blocked at room temperature in 3% hydrogen peroxide in methanol, and permeabilized in 0.1% sodium citrate/0.1% Triton X. Each section was further incubated in 1:7.5 dilution TUNEL reaction mix, at 37°C for 1h followed by incubation with streptavidin-POD enzyme conjugate at 37°C for 30 min. After washes in PBS, Tyramide Signal Amplification was administered and incubated in the dark for 30 min, followed by staining with 4',6-diamidino-2-phenylindole (DAPI) to identify nuclei. TUNEL positive nuclei inside and

outside the dystrophin stain were counted using a Zeiss Observer.D1 microscope with Axiovision image analysis software (Zeiss, Thornwood, NY). Nuclei were considered positive when the TUNEL stain overlapped with DAPI and were considered inside the fiber when the largest part of the DAPI stain was inside the dystrophin outline. Apoptotic nuclear number was presented as the number of TUNEL positive nuclei per 100 muscle fibers.

Caspase Activity

Enzymatic activities of caspase-3, −8, −9 and −12 were measured in the cytosolic fraction as described previously (Leeuwenburgh et al. 2005; McMullen et al. 2009; Xiao et al. 2011). Caspase −3, −8, −9 activities were measured using 7-Amino-4-methlcoumarin (AMC) fluorogenic substrates: Ac-IETD-AMC (caspase-8), Ac-LEHD-AMC, (caspase-9) and Ac-DEVD-AMC (caspase-3), (Peptides International, Louisville, KY). Caspase −12 activity was measured using 7-Amino-4-(trifluoromethyl) coumarin (AFC) fluorogenic substrate Ac-ATAD-AFC (MBL International, Louisville, KY). The substrates are cleaved proteolytically by the corresponding caspases and the fluorescence of free AMC (caspase-3, −8, and −9) and AFC (caspase-12) was measured and compared to a standard curve for free AMC (Sigma, St. Louis, MO) and AFC (Calbiochem, San Diego, CA), respectively. For each reaction, equal amounts of protein were mixed with 1 μM of specific caspase substrate and assay buffer (100 mM HEPES (pH 7.4), 10 mM DTT, 0.1% CHAPS, and 10% sucrose) followed by incubation at 37C for 3 hrs. Liberation of free AMC or AFC from the fluorogenic substrates was detected using a Spectra Max fluorescent microplate reader (Molecular Devices), with an excitation wavelength of 380 nm and an emission wavelength of 460 nm for AMC and excitation of 400 and emission 505nm for AFC. Caspase activity for caspase-12 was measured using 200 μg of protein while the other caspases were assessed using 100 μg. Therefore, caspase activities were expressed as nmoles AMC or AFC per unit of protein.

Western Blotting

Western blot analysis was performed as described previously with minor modifications (McMullen et al. 2009). Western blots were used to measure protein abundance of heat shock proteins 27 and 70 (HSP27 and HSP70), endonuclease G (EndoG), Apoptosis Repressor with CARD domain (ARC), and apoptosis inducing factor (AIF). Protein from CF and/or NF (40μg for HSPs, AIF, ARC; 100μg for EndoG) was loaded and separated on 4–15% Tris-HCl acrylamide gel (BioRad, Hercules, CA); protein was transferred to PVDF membrane (Millipore, Billerica, MA), blocked overnight at 4C in blocking buffer (Li-Cor, Lincoln, NE), and incubated in primary antibody as follows: ARC (1:200; ProSci Incorporated, Poway, CA), HSP27 (1:2000; Enzo Life Sciences, Plymouth, PA), HSP70 (1:500; Cell Signaling, Danvers, MA), EndoG (1:500; Millipore, Billerica, MA), or AIF (1:200; Santa Cruz Biotechnologies, Santa Cruz, CA) overnight at 4C. Membranes were then incubated with highly cross-absorbed infra red-labeled secondary antibodies (1:30,000; Li-Cor) for 20 min at room temperature. Membranes were scanned using Odyssey infrared imaging system (Li-Cor) to detect specific antibody binding and quantification was performed using Odyssey software. Since no single protein could be used to ensure equal loading between the cytosolic and nuclear fractions from the different samples, we used Ponceau S on every gel (data not shown, Sigma-Aldrich, St. Louis, MO).

Immunoprecipitations (IP)

IP were performed according to the manufacturer's protocol using the Immunoprecipitation kit-Dynabeads Protein G (Invitrogen). Briefly, Dynabeads Protein G were bound to 10 μg HSP70 antibody (Cell Signaling, Danvers, MA) for 40 min at room temperature. Crosslinking of Dynabeads to the antibody was performed using BS^3 Crosslinkers to prevent elution of Ig from the complex (Thermo Scientific, Rockford, IL). After crosslinking 25 μg of soleus or TA cytosolic fractions were added to the Dynabeads and incubated with rotation for 90 min. Dynabeads were then collected with a magnet and the supernatant was discarded. Protein from the Dynabeads was eluded using Elution Buffer, supplied in the kit, with equal amounts of Laemlli and SDS buffer. Sample was placed in a heat block 5 min at 95°C, supernatant was separated by magnet and loaded onto a gel for Western blot analysis for detection of cleaved and uncleaved caspase-3 (Cell Signaling, Boston, MA).

Statistics

All statistical analyses were performed using SigmaStat software. Comparisons between two groups were performed using a Student's t-test. A rank sum test was applied when the equal variance test failed (which was the case for caspase activities for TA muscle). When warranted for the comparison of between muscles and treatment groups a Two-way ANOVA was performed and main effects as well as interaction effects are reported as appropriate. In case of statistically significant differences the Holm-Sidak pairwise multiple comparison procedure was employed to determine which groups were different. All values reported are means ± SE and statistical significance was assumed at $p<0.05$.

Results

Muscle weights for TA and soleus were decreased significantly by 56% and 47%, respectively, in rats subjected to DSIM when averaged over the two sets of rats (Table 1). To investigate whether apoptosis was increased in muscles undergoing severe atrophy in response to DSIM two indicators of DNA fragmentation were measured: cytosolic mono- and oligonucleosomal content (apoptotic index, Figure 1A) and TUNEL staining (Figure 1B–E). The apoptotic index was increased 4.2- and 3.6-fold in TA and soleus, respectively, (Figure 1A) as measured by ELISA. TUNEL positive nuclei outside the muscle fibers (interstitial cells) were increased 3.6-and 4.8-fold for TA and soleus, respectively, and TUNEL positive myofiber nuclei were increased by 6.1- and 2.3-fold for TA and soleus muscle, respectively. These data show that apoptosis inside muscle fibers as well as in the interstitial space is elevated in muscles undergoing atrophy associated with DSIM. To investigate which apoptotic pathways are involved with the observed apoptosis in TA and soleus muscles in response to DSIM, we examined caspase-3, −8, −9, and −12 activities in cytosolic fractions. Caspase −3, and −8, but not caspase-9 and −12 activities were elevated significantly in TA muscle with DSIM (Figure 2A), indicating that the extrinsic pathway of apoptosis is activated in this muscle. By contrast, activities of caspase-3, −8, −9, and −12 were not changed in soleus muscles undergoing atrophy in response to DSIM (Figure 2B), although it is interesting to note that caspase-8 activity was higher in soleus in control soleus muscle compared to TA. These results indicate that caspase-dependent apoptotic signaling plays a role in TA, but not in soleus muscle. Since caspase activity was not increased in

soleus muscle despite an increase in apoptosis, we investigated known inhibitors of caspases for their abundance in both muscles. We examined the protein abundance of two heat shock proteins (HSP27 and HSP70), which have been shown to inhibit caspase activity (Garrido et al. 2001; Voss et al. 2007). DSIM was not associated with a change in protein abundance of HSP27 or HSP70 in either muscle, but the abundance of HSP27 and HSP70 protein was 5.3- and 11.1-fold greater, respectively, in soleus than in TA muscle (Figure 3A, B, & C). This suggests that the high levels of HSPs in soleus may inhibit caspases in this muscle, specifically. To examine whether a physical interaction exists between HSP70 and the main executioner caspase, caspase-3, an immunoprecipitation (IP) assay was performed using HSP70 antibody followed by immunoblotting with cleaved (data not shown) and uncleaved caspase-3 antibody in both TA and soleus muscles (Figure 3D). We detected uncleaved, but not cleaved, caspase-3 after IP with HSP70 in both TA and soleus (Figure 3D), indicating HSP70 is directly associated with caspase-3. We further investigated the protein abundance of ARC, a muscle specific inhibitor of caspase-3 and −8 in particular, which was not statistically different between TA and soleus, overall. There was, however, a statistically significant decrease in ARC protein abundance following DSIM in soleus muscle (Figure 4). Since no change in caspases was observed in soleus muscle this decrease with DSIM might indicate a caspase-independent mechanisms of ARC action. In light of increased apoptosis, but no change in caspase activities in soleus muscles, we investigated whether caspase-independent mechanisms were involved in the induction of apoptosis in either TA or soleus. EndoG and AIF protein abundance was measured in cytosolic and nuclear fractions as both proteins translocate from the cytosol to the nucleus upon induction of apoptosis (Kim et al. 2005; Quadrilatero et al. 2011). EndoG abundance did not change with DSIM in either nuclear or cytosolic fractions of TA or soleus muscle indicating that it is likely not involved in the elevation of apoptosis (Figure 5A, B). AIF protein abundance was decreased in the cytosolic fraction of TA muscles with DSIM treatment, but there was no concomitant increase in nuclear AIF, indicating that there is an overall decrease of AIF, but it is not involved in the induction of apoptosis in TA (Figure 5A, C). Similarly, AIF does not appear to be involved in apoptosis in soleus muscle, since no change with DSIM treatment was observed in AIF abundance in either cytosolic or nuclear fractions (Figure 5A, C).

Discussion

The goal of this study was to investigate the role of apoptosis in muscle atrophy for different muscles in a rat model of CIM. We found that DSIM induced substantial muscle atrophy accompanied by significant induction of apoptosis in both TA and soleus muscles. Apoptotic nuclei were observed both inside the muscle fiber as well as in interstitial cells, similar to what has been shown in other atrophy models (Leeuwenburgh et al. 2005). This increase in apoptosis has also been observed in atrophied human quadriceps muscle of patients with CIM in which significant TUNEL staining was found in addition to elevated staining of apoptosis-related proteases, such as caspases (Di Giovanni et al. 2000); furthermore, apoptotic activation was shown to be unique to patients with CIM (Di Giovanni et al. 2000; Di Giovanni et al. 2004) and seemed to be specifically associated with the TGFβ/MAPK pathway (Di Giovanni et al. 2004). In a rat model of CIM which is very similar to ours, it was shown that GADD45 (a growth arrest gene, elevated during apoptosis (Yang et al.

2000)), was elevated, mimicking the human situation (Di Giovanni et al. 2004). More recently, microarray analysis indicated that apoptosis-related genes were differentially expressed in gastrocnemius muscles from rats undergoing procedures closely resembling CIM in humans (Llano-Diez et al. 2011). This study indicated that there is a time-dependent regulation of genes involved in apoptosis such that pro-apoptotic genes were upregulated before the caspase-cascade was activated (Llano-Diez et al. 2011). Interestingly therefore, muscle atrophy occurs before the activation of apoptosis-related pathways in the rat CIM model, which is different from pure disuse models, such as hind limb suspension (Dupont-Versteegden et al. 2006), indicating that interventions for the different forms of atrophy most likely will require distinct strategies. Therefore, data from our study and previous work indicates that apoptosis plays a role in the observed muscle atrophy in CIM and DSIM.

Our results further indicate that muscles with different fiber type composition underwent apoptosis through distinct mechanisms even though the amount of muscle atrophy and the extent of apoptosis were very similar; TA muscles are composed of mainly type II muscle fibers while soleus is almost solely composed of type I fibers (Delp and Duan 1996). In TA muscles apoptosis was accompanied by an increase in caspase-3 and −8, which was not the case for soleus muscle in which these enzymes were not elevated under severe atrophy conditions associated with DSIM. It has been shown previously that apoptosis-related proteins are differentially expressed in muscles with different fiber types as well as in fibers with different myosin heavy chain (MyHC) composition within the same muscle (Braga et al. 2008; McMillan and Quadrilatero 2011; Plomgaard et al. 2005). In general, higher levels of apoptosis-associated proteins are found in muscle composed of type I fibers and in type I compared to type II fibers within the same muscle. McMillan and Quadrilatero (McMillan and Quadrilatero 2011) showed that ARC, AIF, Bax, Bcl-2, cytochrome-c, and Smac, but not XIAP, were elevated in red compared to white gastrocnemius muscle as were caspase-3, −8 and −9 and calpain activities; two other studies showed differential expression of TNFα, Bax and Bcl-2 between fiber types (Braga et al. 2008; Plomgaard et al. 2005). In these studies levels of proteins were measured in a non-perturbed muscle and the data indicate that there may be differences in apoptotic signaling pathways between different muscle fiber types at rest. However, it is known that the actual number of nuclei undergoing apoptosis in a resting muscle is very low and it is uncertain how these differences in apoptotic signaling molecules at basal level influence muscles undergoing some stressor or disease. In two studies it was found that apoptotic signaling was higher in soleus than in TA muscles of rats subjected to angiotensin II (Burniston et al. 2005b) as well as clenbuterol (Burniston et al. 2005a), indicating that separate muscles indeed respond differently to stressors. In our current study we show for the first time that the fiber type specific differences in apoptosis signaling also exist for muscles undergoing severe atrophy during DSIM.

One of the possible reasons caspase activities were not elevated with DSIM in soleus in contrast to TA muscle is that anti-apoptotic proteins are higher in muscles with a predominance of type I fibers. HSPs are cell protective proteins induced in response to stress, and HSP-27 and −70, in particular, are potent anti-apoptotic proteins (Garrido et al. 2001); their mode of action is still under investigation, but includes direct binding to caspases (Voss et al. 2007). HSP70 is expressed to much higher extent in slow oxidative compared to fast glycolytic muscle fibers (Locke et al. 1991; McMillan and Quadrilatero

2011; Neufer et al. 1996; O'Neill et al. 2006) and it has been suggested that this is a compensatory response for slow muscles being in a more pro-apoptotic state (McMillan and Quadrilatero 2011). Interestingly, masticatory muscles show elevated levels of HSPs in CIM models and are spared from muscle atrophy, but whether this is due to decreased levels of apoptosis was not investigated (Aare et al. 2011; Akkad et al. 2014). In this study we also showed that HSP27 and HSP70 were substantially higher in soleus versus TA muscle and additionally that HSP70 is physically associated with uncleaved caspase-3. Since the level of HSP70 in soleus is significantly higher than in TA muscle, this binding might inhibit caspase-3 activity in soleus, but to a lesser extent in TA. In addition to the higher abundance of HSPs in slow compared to fast muscle, the anti-apoptotic protein ARC is also highly elevated in soleus (McMillan and Quadrilatero 2011). ARC is a potent anti-apoptotic protein in postmitotic cells which is capable of regulating apoptosis through the extrinsic and intrinsic pathways as well as affecting the endoplasmic reticulum mediated apoptosis pathway (reviewed in (Ludwig-Galezowska et al. 2011)). Interestingly, ARC protein abundance was decreased with DSIM in soleus only and may be involved in the elevated apoptosis in this muscle, while its role in TA is not changed with DSIM. Thus, we suggest that the anti-apoptotic mechanisms (HSPs and ARC) in soleus are inhibiting caspases, while TA does not have this protection and therefore has elevated caspase activities. However, despite the lack of increase in caspase activities, apoptosis is still highly elevated in soleus muscle with DSIM and we propose that the mechanisms responsible for this increase are likely caspase-independent. We investigated two mitochondrial proteins involved in caspase-independent apoptosis in muscles, AIF and EndoG. However, we found that the nuclear protein levels of these proteins were not changed with DSIM and therefore we conclude that they are not involved in the apoptotic response in this model at this time point. The mechanisms or proteins responsible for the elevated levels of apoptosis in soleus muscle therefore remain to be determined.

It has to be noted that the muscles in this study were taken fairly late in the process of atrophy and therefore early changes in apoptosis-related events may have been missed. We showed previously that EndoG translocation is an early event during disuse atrophy (Dupont-Versteegden et al. 2006) and the fact that we did not see differences in this variable or in AIF localization may indicate that the time point of tissue collection was not optimal to measure these proteins. Indeed, Llano-Diez et al. (Llano-Diez et al. 2011) show that the expression of atrophy and apoptosis genes in a CIM model is highly regulated in a unique and coordinated temporal fashion in which caspase related events occur fairly late in the process. We extend this finding to show that the regulation of apoptosis is also muscle specific and it will need to be determined whether muscles of different fiber types undergo apoptosis at a different rate rather than through different mechanisms.

The findings in this paper have important implications for developing interventions to combat apoptosis and the potentially associated atrophy that accompanies CIM. Since separate mechanisms are associated with apoptosis in different muscles, potentially in a distinct temporal pattern, therapies will have to be developed that address all processes involved. Inhibition of only caspases, for example, will not suffice to decrease apoptosis in muscles of all fiber types and alleviate symptoms associated with elevated apoptosis and atrophy. We suggest that one of the interventions that would be advantageous is physical

exercise training; while acute strenuous exercise is generally pro-apoptotic, regular exercise training has been shown to decrease DNA fragmentation and pro-apoptotic signaling (for review(Quadrilatero et al. 2011)). A recent study showed that aerobic training in hypertensive rats inhibited the elevation of pro-apoptotic proteins usually involved with caspase activation as well as induction of caspase-independent pathways (McMillan et al. 2012), and therefore could influence apoptosis initiated by multiple processes and in different muscles. However, physical exercise is only feasible in patients who are ambulatory and may therefore not be an intervention that can be used in the clinical population until after discharge from the ICU, indicating that other interventions need to be investigated.

In summary, this study shows that severe atrophy with DSIM is accompanied by a significant increase in apoptosis and apoptosis-related signaling pathways, which are differentially regulated in muscles with distinct fiber type composition. Anti-apoptotic proteins elevated in type I fibers may decrease caspase activation specifically, but do not inhibit the extent of apoptosis or atrophy with DSIM and therefore other mechanisms need to be identified for apoptosis occurring in type I fibers. Consequently, interventions to combat apoptosis-related atrophy in patients with CIM need to be targeted to caspase-dependent as well as independent processes.

Acknowledgments

The authors would like to thank Gregory Filatov and Kevin Novak for technical assistance. This work was supported by NIH grant# NS082354 (MMR) and an Undergraduate Summer Research Fellowship from the American Physiological Society (BTB).

Literature Cited

Aare S, et al. Mechanisms underlying the sparing of masticatory versus limb muscle function in an experimental critical illness model. Physiol Genomics. 2011; 43:1334–1350. [PubMed: 22010006]

Akkad H, Corpeno R, Larsson L. Masseter muscle myofibrillar protein synthesis and degradation in an experimental critical illness myopathy model. PLoS One. 2014; 9:e92622. [PubMed: 24705179]

Banduseela VC, et al. Gene expression and muscle fiber function in a porcine ICU model. Physiol Genomics. 2009; 39:141–159. [PubMed: 19706692]

Batt J, dos Santos CC, Cameron JI, Herridge MS. Intensive care unit-acquired weakness: clinical phenotypes and molecular mechanisms. Am J Respir Crit Care Med. 2013; 187:238–246. [PubMed: 23204256]

Bhatnagar S, Mittal A, Gupta SK, Kumar A. TWEAK causes myotube atrophy through coordinated activation of ubiquitin-proteasome system, autophagy, and caspases. J Cell Physiol. 2012; 227:1042–1051. [PubMed: 21567392]

Boivin MA, et al. Activation of caspase-3 in the skeletal muscle during haemodialysis. Eur J Clin Invest. 2010; 40:903–910. [PubMed: 20636378]

Bolton CF. Neuromuscular manifestations of critical illness. Muscle Nerve. 2005; 32:140–163. [PubMed: 15825186]

Braga M, et al. Involvement of oxidative stress and caspase 2-mediated intrinsic pathway signaling in age-related increase in muscle cell apoptosis in mice. Apoptosis. 2008; 13:822–832. [PubMed: 18461459]

Bruusgaard JC, Egner IM, Larsen TK, Dupre-Aucouturier S, Desplanches D, Gundersen K. No change in myonuclear number during muscle unloading and reloading. J Appl Physiol. 2012; 113:290–296. [PubMed: 22582213]

Bruusgaard JC, Gundersen K. In vivo time-lapse microscopy reveals no loss of murine myonuclei during weeks of muscle atrophy. J Clin Invest. 2008; 118:1450–1457. [PubMed: 18317591]

Burniston JG, Chester N, Clark WA, Tan LB, Goldspink DF. Dose-dependent apoptotic and necrotic myocyte death induced by the beta2-adrenergic receptor agonist, clenbuterol. Muscle Nerve. 2005a; 32:767–774. [PubMed: 16007677]

Burniston JG, Saini A, Tan LB, Goldspink DF. Angiotensin II induces apoptosis in vivo in skeletal, as well as cardiac, muscle of the rat. Exp Physiol. 2005b; 90:755–761. [PubMed: 15987733]

Delp MD, Duan C. Composition and size of type I, IIA, IID/X, and IIB fibers and citrate synthase activity of rat muscle. J Appl Physiol. 1996; 80:261–270. [PubMed: 8847313]

Di Giovanni S, Mirabella M, D'Amico A, Tonali P, Servidei S. Apoptotic features accompany acute quadriplegic myopathy. Neurology. 2000; 55:854–858. [PubMed: 10994008]

Di Giovanni S, Molon A, Broccolini A, Melcon G, Mirabella M, Hoffman EP, Servidei S. Constitutive activation of MAPK cascade in acute quadriplegic myopathy. Ann Neurol. 2004; 55:195–206. [PubMed: 14755723]

Du J, et al. Activation of caspase-3 is an initial step triggering accelerated muscle proteolysis in catabolic conditions. J Clin Invest. 2004; 113:115–123. [PubMed: 14702115]

Dupont-Versteegden EE. Apoptosis in muscle atrophy: relevance to sarcopenia. Experimental Gerontology. 2005; 40:473–481. [PubMed: 15935591]

Dupont-Versteegden EE, Murphy RJ, Houle JD, Gurley CM, Peterson CA. Activated satellite cells fail to restore myonuclear number in spinal cord transected and exercised rats. Am J Physiol. 1999; 277:C589–C597. [PubMed: 10484346]

Dupont-Versteegden EE, Strotman BA, Gurley CM, Gaddy D, Knox M, Fluckey JD, Peterson CA. Nuclear translocation of EndoG at the initiation of disuse muscle atrophy and apoptosis is specific to myonuclei. Am J Physiol Regul Integr Comp Physiol. 2006; 291:R1730–R1740. [PubMed: 16873557]

Eley HL, Russell ST, Tisdale MJ. Mechanism of attenuation of muscle protein degradation induced by tumor necrosis factor-alpha and angiotensin II by beta-hydroxy-beta-methylbutyrate. Am J Physiol Endocrinol Metab. 2008; 295:E1417–E1426. [PubMed: 18840762]

Garrido C, Gurbuxani S, Ravagnan L, Kroemer G. Heat shock proteins: endogenous modulators of apoptotic cell death. Biochem Biophys Res Commun. 2001; 286:433–442. [PubMed: 11511077]

Gundersen K, Bruusgaard JC. Nuclear domains during muscle atrophy: nuclei lost or paradigm lost? J Physiol. 2008; 586:2675–2681. [PubMed: 18440990]

Helliwell TR, Wilkinson A, Griffiths RD, McClelland P, Palmer TE, Bone JM. Muscle fibre atrophy in critically ill patients is associated with the loss of myosin filaments and the presence of lysosomal enzymes and ubiquitin. Neuropathol Appl Neurobiol. 1998; 24:507–517. [PubMed: 9888161]

Kim R, Emi M, Tanabe K. Caspase-dependent and -independent cell death pathways after DNA damage (Review). Oncol Rep. 2005; 14:595–599. [PubMed: 16077961]

Kraner SD, Wang Q, Novak KR, Cheng D, Cool DR, Peng J, Rich MM. Upregulation of the CaV 1.1-ryanodine receptor complex in a rat model of critical illness myopathy. Am J Physiol Regul Integr Comp Physiol. 2011; 300:R1384–R1391. [PubMed: 21474431]

Lacomis D, Zochodne DW, Bird SJ. Critical illness myopathy. Muscle Nerve. 2000; 23:1785–1788. [PubMed: 11102901]

Latronico N, Bolton CF. Critical illness polyneuropathy and myopathy: a major cause of muscle weakness and paralysis. Lancet Neurol. 2011; 10:931–941. [PubMed: 21939902]

Lee MC, Wee GR, Kim JH. Apoptosis of skeletal muscle on steroid-induced myopathy in rats. J Nutr. 2005; 135:1806S–1808S. [PubMed: 15987869]

Leeuwenburgh C, Gurley CM, Strotman BA, Dupont-Versteegden EE. Age-related differences in apoptosis with disuse atrophy in soleus muscle. Am J Physiol Regul Integr Comp Physiol. 2005; 288:R1288–R1296. [PubMed: 15650125]

Llano-Diez M, Gustafson AM, Olsson C, Goransson H, Larsson L. Muscle wasting and the temporal gene expression pattern in a novel rat intensive care unit model. BMC Genomics. 2011; 12:602. [PubMed: 22165895]

Locke M, Noble EG, Atkinson BG. Inducible isoform of HSP70 is constitutively expressed in a muscle fiber type specific pattern. Am J Physiol. 1991; 261:C774–C779. [PubMed: 1951668]

Ludwig-Galezowska AH, Flanagan L, Rehm M. Apoptosis repressor with caspase recruitment domain, a multifunctional modulator of cell death. J Cell Mol Med. 2011; 15:1044–1053. [PubMed: 21129150]

Massa R, Carpenter S, Holland P, Karpati G. Loss and renewal of thick myofilaments in glucocorticoid-treated rat soleus after denervation and reinnervation. Muscle Nerve. 1992; 15:1290–1298. [PubMed: 1488068]

McMillan EM, Graham DA, Rush JW, Quadrilatero J. Decreased DNA fragmentation and apoptotic signaling in soleus muscle of hypertensive rats following 6 weeks of treadmill training. J Appl Physiol. 2012; 113:1048–1057. (1985). [PubMed: 22858629]

McMillan EM, Quadrilatero J. Differential apoptosis-related protein expression, mitochondrial properties, proteolytic enzyme activity, and DNA fragmentation between skeletal muscles. Am J Physiol Regul Integr Comp Physiol. 2011; 300:R531–R543. [PubMed: 21148478]

McMullen CA, Ferry AL, Gamboa JL, Andrade FH, Dupont-Versteegden EE. Age-related changes of cell death pathways in rat extraocular muscle. Exp Gerontol. 2009; 44:420–425. [PubMed: 19341788]

Mozaffar T, Haddad F, Zeng M, Zhang LY, Adams GR, Baldwin KM. Molecular and cellular defects of skeletal muscle in an animal model of acute quadriplegic myopathy. Muscle Nerve. 2007; 35:55–65. [PubMed: 16967495]

Nelson WB, Smuder AJ, Hudson MB, Talbert EE, Powers SK. Cross-talk between the calpain and caspase-3 proteolytic systems in the diaphragm during prolonged mechanical ventilation. Crit Care Med. 2012; 40:1857–1863. [PubMed: 22487998]

Neufer PD, Ordway GA, Hand GA, Shelton JM, Richardson JA, Benjamin IJ, Williams RS. Continuous contractile activity induces fiber type specific expression of HSP70 in skeletal muscle. Am J Physiol. 1996; 271:C1828–C1837. [PubMed: 8997182]

O'Neill DE, Aubrey FK, Zeldin DA, Michel RN, Noble EG. Slower skeletal muscle phenotypes are critical for constitutive expression of Hsp70 in overloaded rat plantaris muscle. J Appl Physiol. 2006; 100:981–987. (1985). [PubMed: 16293703]

Orzechowski A, Jank M, Gajkowska B, Sadkowski T, Godlewski MM, Ostaszewski P. Delineation of signalling pathway leading to antioxidant-dependent inhibition of dexamethasone-mediated muscle cell death. Journal of muscle research and cell motility. 2003; 24:33–53. [PubMed: 12953835]

Plomgaard P, Penkowa M, Pedersen BK. Fiber type specific expression of TNF-alpha, IL-6 and IL-18 in human skeletal muscles. Exercise immunology review. 2005; 11:53–63. [PubMed: 16385844]

Quadrilatero J, Alway SE, Dupont-Versteegden EE. Skeletal muscle apoptotic response to physical activity: potential mechanisms for protection. Appl Physiol Nutr Metab. 2011; 36:608–617. [PubMed: 21936642]

Rich MM, Pinter MJ. Sodium channel inactivation in an animal model of acute quadriplegic myopathy. Ann Neurol. 2001; 50:26–33. [PubMed: 11456306]

Rich MM, Pinter MJ. Crucial role of sodium channel fast inactivation in muscle fibre inexcitability in a rat model of critical illness myopathy. J Physiol. 2003; 547:555–566. [PubMed: 12562930]

Rich MM, Pinter MJ, Kraner SD, Barchi RL. Loss of electrical excitability in an animal model of acute quadriplegic myopathy. Ann Neurol. 1998; 43:171–179. [PubMed: 9485058]

Rouleau G, Karpati G, Carpenter S, Soza M, Prescott S, Holland P. Glucocorticoid excess induces preferential depletion of myosin in denervated skeletal muscle fibers. Muscle Nerve. 1987; 10:428–438. [PubMed: 3614257]

Russell ST, Rajani S, Dhadda RS, Tisdale MJ. Mechanism of induction of muscle protein loss by hyperglycaemia. Exp Cell Res. 2009; 315:16–25. [PubMed: 18973755]

Sakuma K, Yamaguchi A. Sarcopenia and cachexia: the adaptations of negative regulators of skeletal muscle mass. J Cachexia Sarcopenia Muscle. 2012

Showalter CJ, Engel AG. Acute quadriplegic myopathy: analysis of myosin isoforms and evidence for calpain-mediated proteolysis. Muscle Nerve. 1997; 20:316–322. [PubMed: 9052810]

Sishi B, Loos B, Ellis B, Smith W, du Toit EF, Engelbrecht AM. Diet-induced obesity alters signalling pathways and induces atrophy and apoptosis in skeletal muscle in a prediabetic rat model. Exp Physiol. 2011; 96:179–193. [PubMed: 20952489]

Siu PM, Pistilli EE, Butler DC, Alway SE. Aging influences cellular and molecular responses of apoptosis to skeletal muscle unloading. Am J Physiol Cell Physiol. 2005; 288:C338–C349. [PubMed: 15483226]

Smuder AJ, Kavazis AN, Hudson MB, Nelson WB, Powers SK. Oxidation enhances myofibrillar protein degradation via calpain and caspase-3 Free Radic. Biol Med. 2010; 49:1152–1160.

Stevens RD, et al. A framework for diagnosing and classifying intensive care unit-acquired weakness. Critical Care Medicine. 2009; 37:S299–S308. [PubMed: 20046114]

Talbert EE, Smuder AJ, Min K, Kwon OS, Powers SK. Calpain and caspase-3 play required roles in immobilization-induced limb muscle atrophy. J Appl Physiol. 2013; 114:1482–1489. (1985). [PubMed: 23471945]

Teng BT, Tam EW, Benzie IF, Siu PM. Protective effect of caspase inhibition on compression-induced muscle damage. J Physiol. 2011; 589:3349–3369. [PubMed: 21540338]

van Royen M, Carbo N, Busquets S, Alvarez B, Quinn LS, Lopez-Soriano FJ, Argiles JM. DNA fragmentation occurs in skeletal muscle during tumor growth: A link with cancer cachexia? Biochem Biophys Res Commun. 2000; 270:533–537. [PubMed: 10753659]

Voss OH, Batra S, Kolattukudy SJ, Gonzalez-Mejia ME, Smith JB, Doseff AI. Binding of caspase-3 prodomain to heat shock protein 27 regulates monocyte apoptosis by inhibiting caspase-3 proteolytic activation. J Biol Chem. 2007; 282:25088–25099. [PubMed: 17597071]

Wang XH, Zhang L, Mitch WE, LeDoux JM, Hu J, Du J. Caspase-3 cleaves specific 19 S proteasome subunits in skeletal muscle stimulating proteasome activity. J Biol Chem. 2010; 285:21249–21257. [PubMed: 20424172]

Xiao R, Ferry AL, Dupont-Versteegden EE. Cell death-resistance of differentiated myotubes is associated with enhanced anti-apoptotic mechanisms compared to myoblasts. Apoptosis. 2011; 16:221–234. [PubMed: 21161388]

Yang Q, Manicone A, Coursen JD, Linke SP, Nagashima M, Forgues M, Wang XW. Identification of a functional domain in a GADD45-mediated G2/M checkpoint. J Biol Chem. 2000; 275:36892–36898. [PubMed: 10973963]

Yasuhara S, et al. Skeletal muscle apoptosis after burns is associated with activation of proapoptotic signals. Am J Physiol Endocrinol Metab. 2000; 279:E1114–E1121. [PubMed: 11052967]

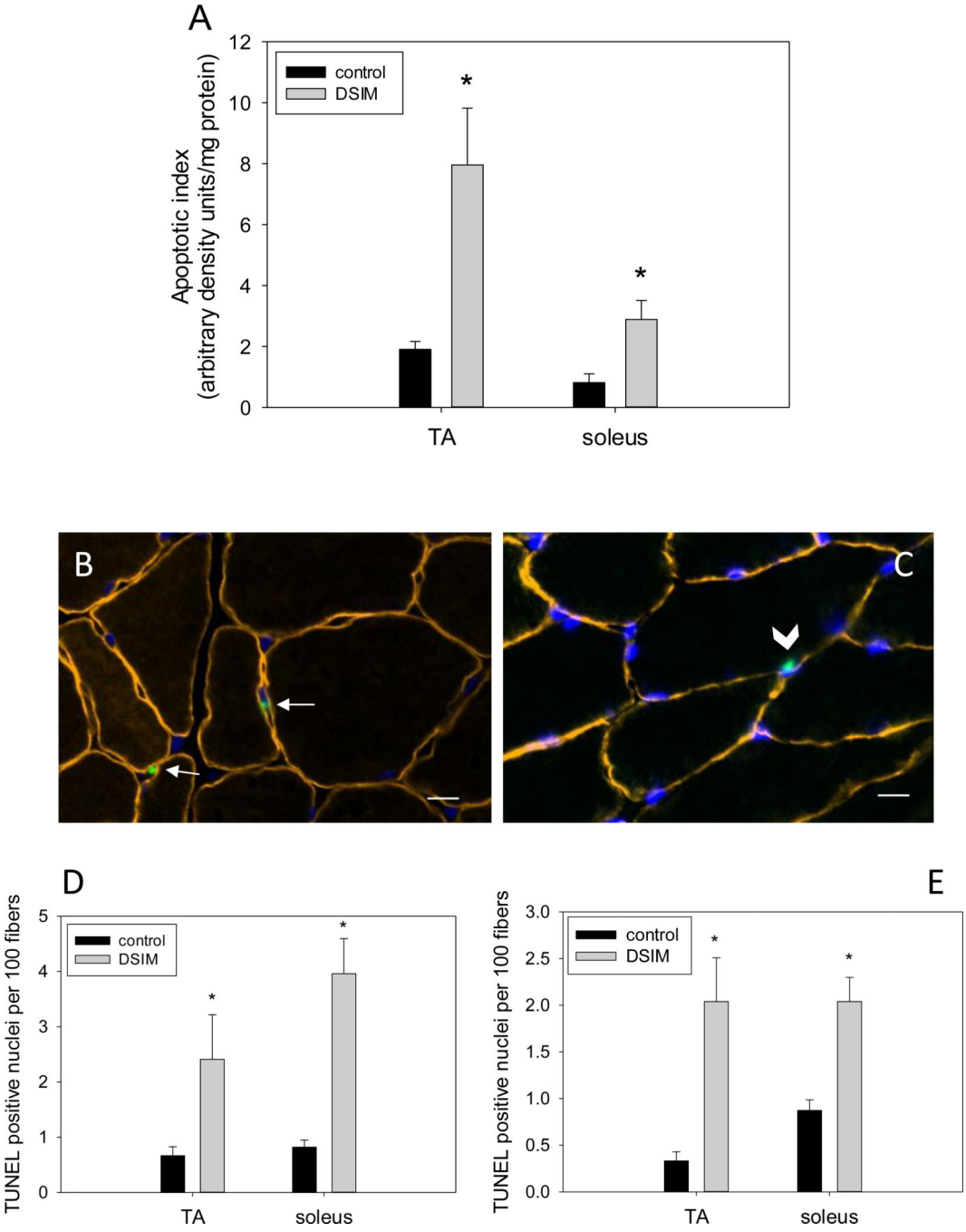

Figure 1. Apoptosis is increased in muscles affected by DSIM

Apoptotic index is depicted in (A). Representative cross sections stained for dystrophin (orange), DAPI (Blue) and TUNEL are shown (B&C); arrows in (B) indicate TUNEL positive nuclei in the interstitial area and arrow head in (C) indicates a TUNEL positive nucleus inside the muscle fiber. Scale bars in (B) and (C) are 10 μm. Quantification of TUNEL staining is shown for nuclei outside (D) and inside (E) the muscle fibers for TA and soleus muscles of control (black bars) and DSIM (grey bars) rats. Values are means ± SE,* indicates statistically significant difference from control within the same muscle, $p<0.05$.

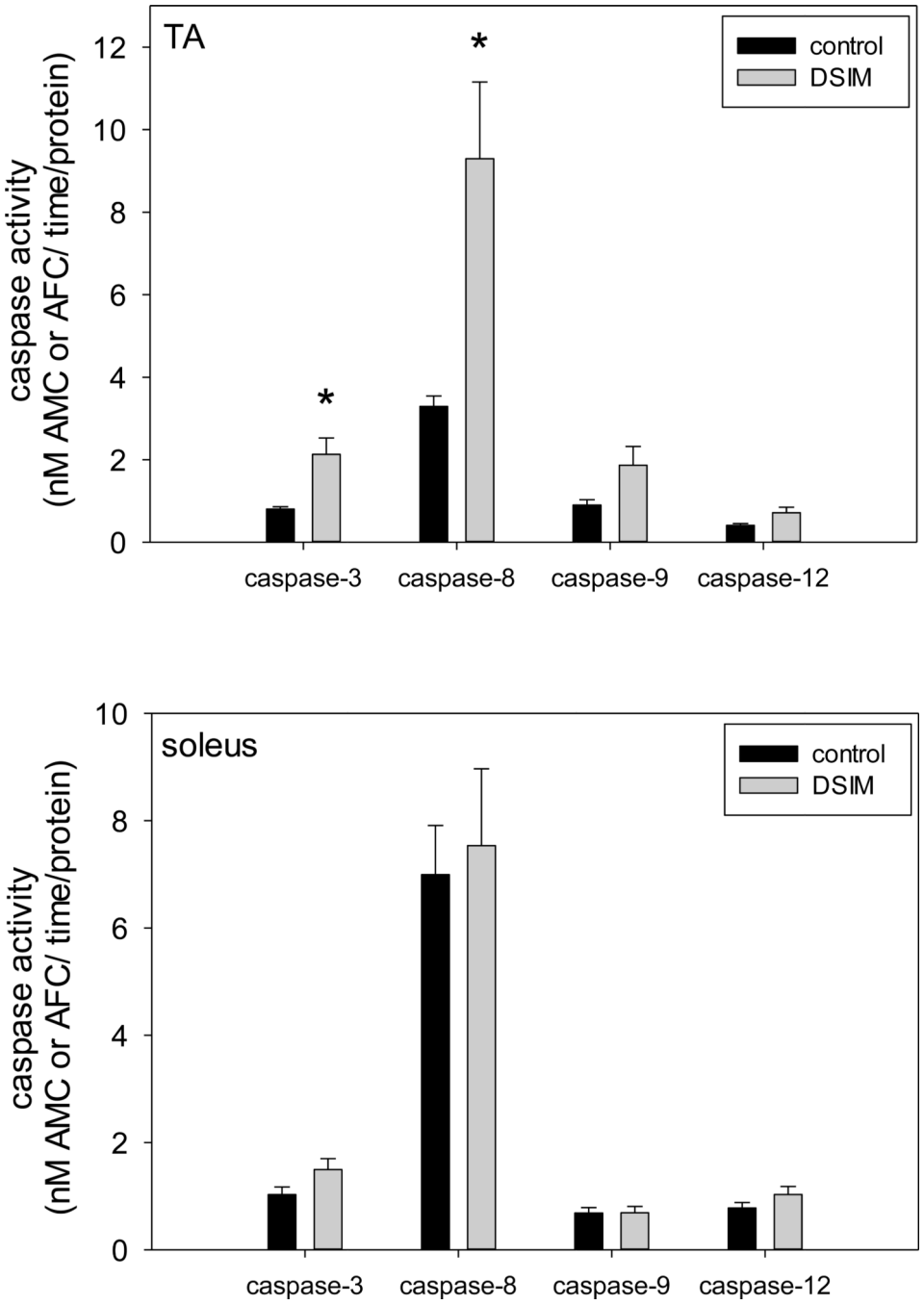

Figure 2. Activation of selected caspases with DSIM in TA muscle only

Activities of caspase-3, −8, −9, and −12 are shown for TA (top panel) and soleus (bottom panel) muscles from control (black bars) and DSIM (grey bars) rats. Values are means ± SE, * indicates statistically significant difference from control within the same muscle, $p<0.05$.

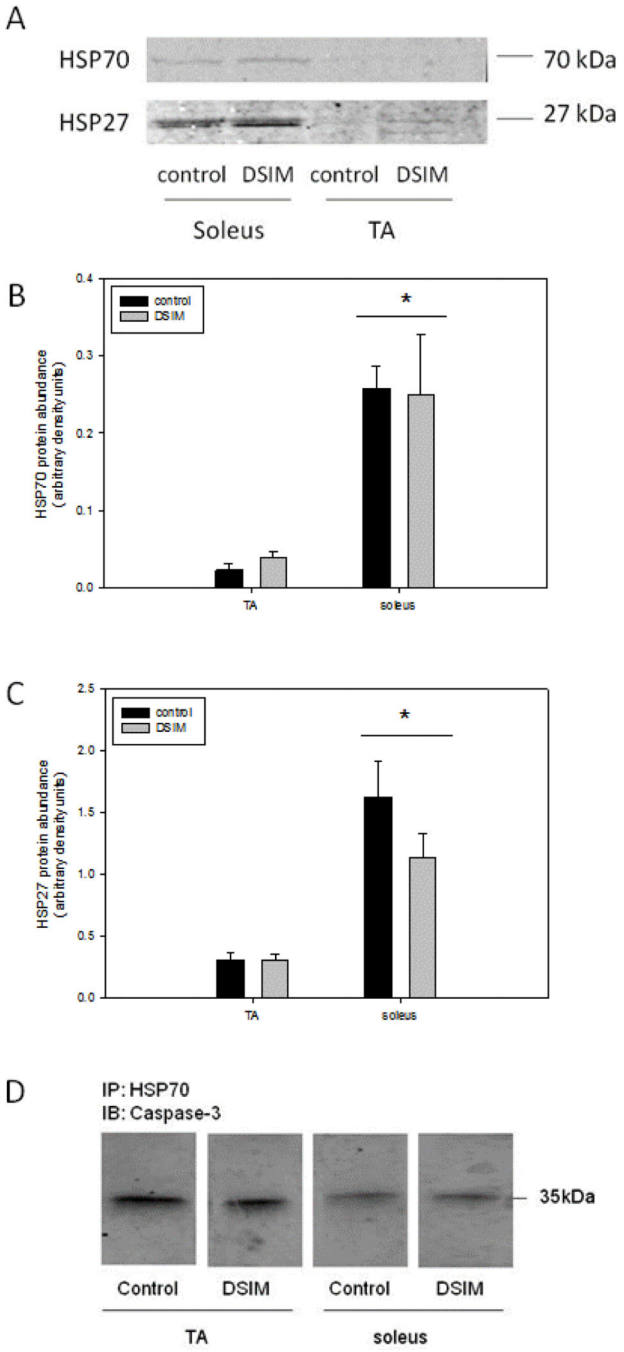

Figure 3. Abundance of heat shock proteins is higher in soleus muscle, but does not change with DSIM

Representative Western blots of HSP 70 (A, top) and HSP27 (A, bottom) protein are shown. Quantification of HSP70 (B) and HSP27 (C) protein abundance in TA and soleus muscles of control (black bars) and DSIM (grey bars) rats is depicted in bar graphs. Values are means ± SE, * indicates statistically significant main effect between TA and soleus muscles. Immunoprecipitation (IP) with HSP70 and immunoblotting (IB) with caspase-3 is shown in (D).

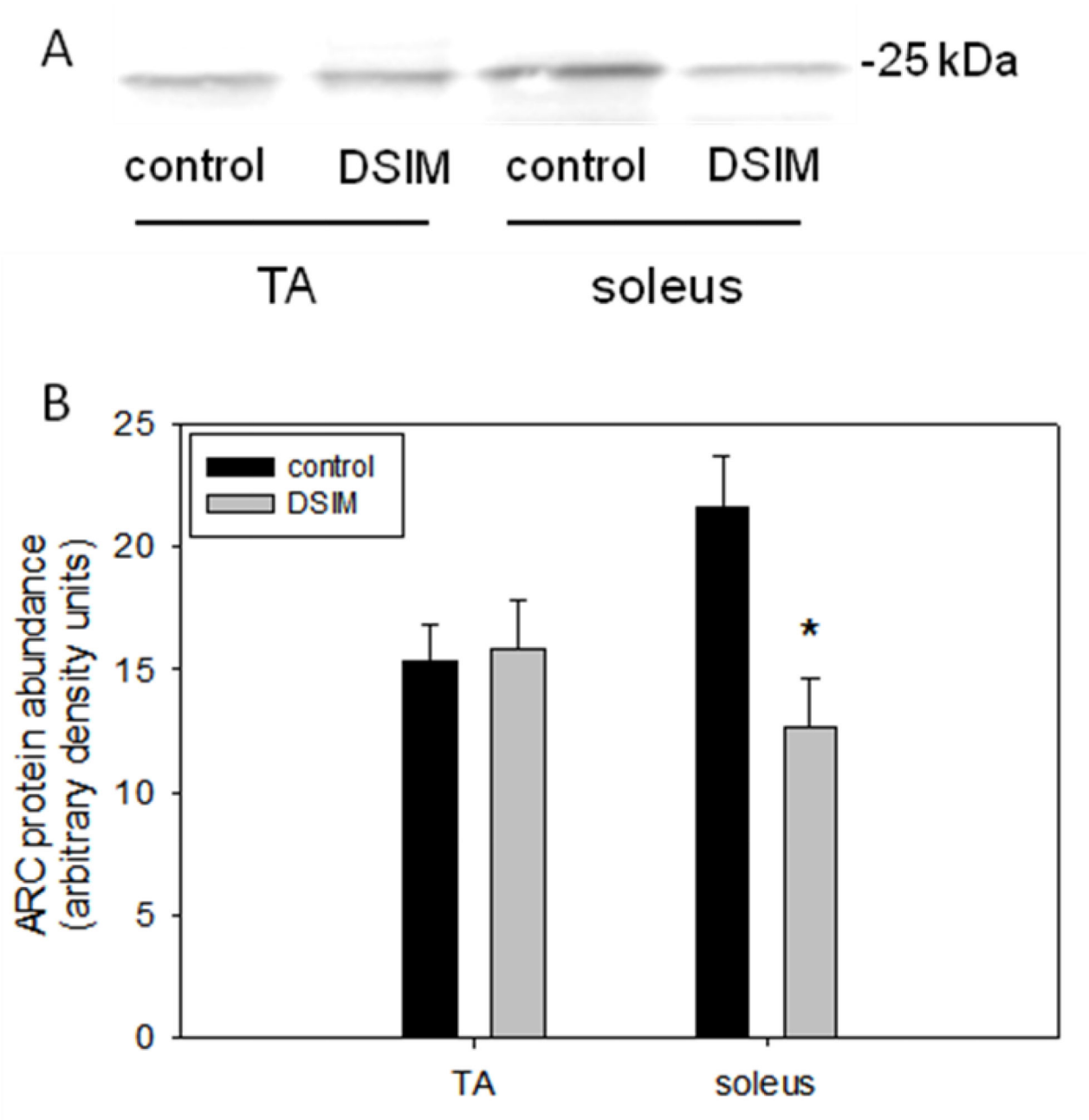

Figure 4. ARC abundance is decreased with DSIM in soleus muscle

Representative Western blot of ARC is shown (A). ARC protein abundance of TA and soleus muscle from control (black bars) and DSIM (grey bars) rats is depicted (B). Values are means ± SE, * indicates significantly different from control within same muscle, $p<0.05$.

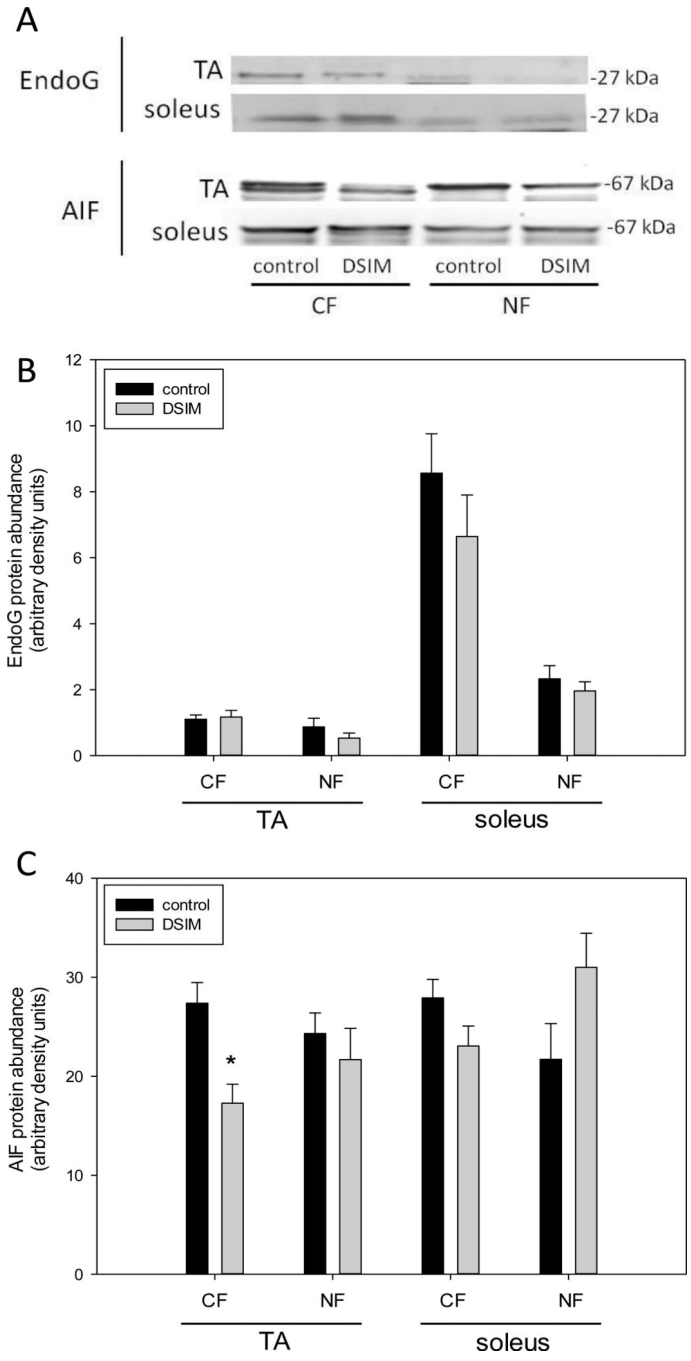

Figure 5. The role of EndoG and AIF in muscle atrophy with DSIM

Representative Western blots of EndoG and AIF in cytosolic (CF) and nuclear (NF) fractions from TA and soleus muscle of control and DSIM rats. Quantification of EndoG (B) and AIF (C) protein abundance of CF and NF in TA and soleus muscles from control (black bars) and DSIM (grey bars) rats. Values are means ± SE, * indicates statistically significant difference from control, $p<0.05$.

Table 1

		muscle weight (mg)	
		control	**DSIM**
set 1	TA	514 ± 10	181 ± 15 *
	soleus	148 ± 5	69 ± 6 *
set 2	TA	512 ± 8	275 ± 9 *
	soleus	153 ± 5	93 ± 6 *

Values are means ± SE

* indicates significantly different from control, $p<0.05$